

## Rotational velocities for the EXPORT sample

E. Solano

*INSA-Laboratorio de Astrofísica Espacial y Física Fundamental.*  
*Apartado de Correos 50727, E-28080 Madrid, Spain*

B. Montesinos

*Laboratorio de Astrofísica Espacial y Física Fundamental. Apartado de*  
*Correos 50727, E-28080, Madrid, Spain*

*Instituto de Astrofísica de Andalucía. Apartado de Correos 3004,*  
*E-18080, Granada, Spain*

A. Mora

*Departamento de Física Teórica, Facultad de Ciencias, Universidad*  
*Autónoma de Madrid, E-28049 Cantoblanco, Madrid, Spain*

EXPORT

### Abstract.

An homogeneous set of projected rotational velocities of the targets observed during the 1998 La Palma International Time campaigns is presented here. This is part of a project whose main goal is to perform a detailed chemical analysis of these objects and to study their implications in the planetary formation phenomenon.

## 1. Introduction

A precise determination of rotational velocities is of fundamental importance to understand the process of planetary formation. Despite this, most of the values published in the literature are based on poor quality data or are affected by systematic errors (e.g., combination of observations with different resolutions or selection of lines broadened by other agents than rotation). These problems are not present in this work where the same instrumentation and observational configuration have been used for all the stars in the sample and a careful selection of lines, where rotation is the only source of broadening, has been made.

## 2. The method

Projected rotational velocities have been measured using the method described in Gray (1992). In short, it is based on the relation between  $v \sin i$  and the frequencies where the Fourier transform of the rotational profile reaches a relative minimum (Figure 1). If the spectral resolution is reasonably high, the instru-

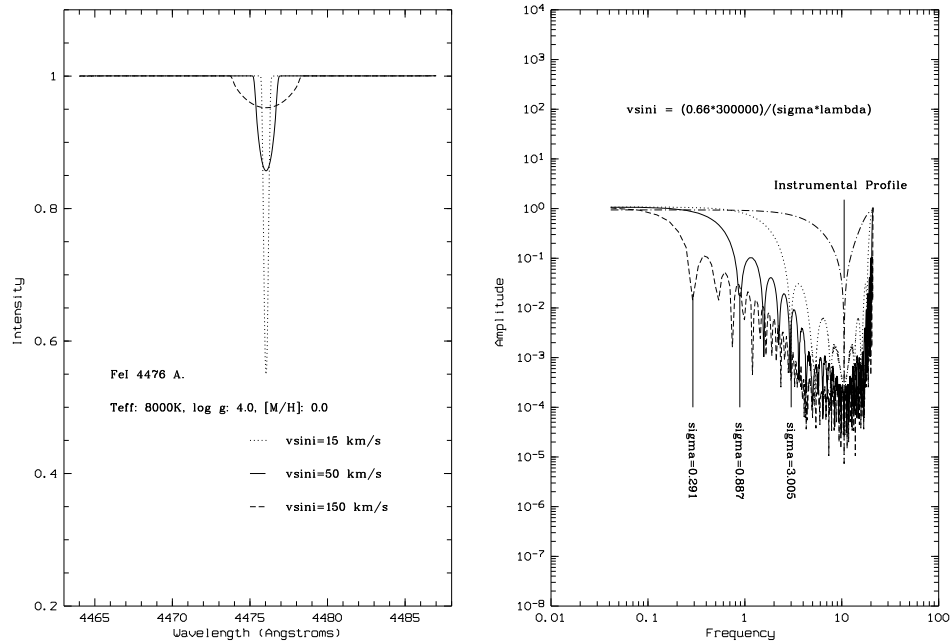


Figure 1. *Left panel:* Influence of rotational broadening on spectral lines. The synthetic line FeI 4476 Å is shown for different broadenings. *Right panel:* Fourier transforms and their relation with rotational velocities.

mental profile may add, at high frequencies, relative minima to the Fourier transform, therefore, not contaminating the transform of the rotational profile (Figure 1, left panel). Projected rotational velocities for our sample of stars are given in Table 1.

Unlike other methods (e.g. Sletteback 1975; Tonry & Davis 1979), the one presented here does not need any *a priori* calibration providing direct and independent measurements of  $v \sin i$ .

The assumptions underlying the method are the following:

- **The star is spherical:** Stars of our sample rotate far below their break-up velocities.
- **The star rotates rigidly:** This is not true for late-type stars but latitudinal differential rotation only affects the high frequency part whereas  $v \sin i$  is calculated from the low frequency region (Bruning 1981).
- **The line profile stays constant along the stellar disk.**

### 3. Macroturbulence

The method used to calculate projected rotational velocities is also valid to determine in slow rotators other sources of broadening like macroturbulence.

The basic assumption is that the observed line profile can be described by the following expression:

$$F(\lambda) = T(\lambda) * I(\lambda) * R(\lambda) * M(\lambda) \quad (1)$$

where  $*$  means convolution or, in the Fourier space, by the product of

$$f(\sigma) = t(\sigma)i(\sigma)r(\sigma)m(\sigma) \quad (2)$$

where

- $F(\lambda)$ : **Observed profile**. To improve the analysis, an averaged profile of several lines with similar depth of formation has been used.
- $T(\lambda)$ : **Thermal profile**. Negligible for moderate-intensity lines.
- $I(\lambda)$ : **Instrumental profile**. Measured from calibration spectra.
- $R(\lambda)$ : **Rotational profile**.
- $M(\lambda)$ : **Macroturbulence profile**.

Macroturbulence can be estimated by simply removing the other sources of broadening. Figure 2 (left panel) shows how the instrumental broadening-free profile (solid) cannot be fitted by a single rotational profile (dotted) suggesting the presence of an additional source of broadening that can be ascribed to macroturbulence (dashed) comparable, in slow rotators, to rotation. This is not the case of fast-rotators where macroturbulence is negligible and the instrumental broadening-free profile (solid) can be suitably fitted by a single rotational profile (dotted) (Figure 2, right panel). Residuals at high frequencies can be ascribed to amplified noise.

#### 4. Estimated uncertainties

- **Continuum placement**: A displacement of the continuum level may change the line profile and thus distort the shape of the Fourier transform modifying the position of the relative minima. This is particularly important for high values of  $v \sin i$  due to the weakening of the line depth.
- **Sampling frequency**: This is another limiting factor in the calculation of  $v \sin i$ . Defining this frequency as  $\sigma_N = 0.5/\Delta\lambda$  and considering the spectral resolution of our observations, the lowest  $v \sin i$  value that can be achieved is  $\approx 4$  km/s. Hence, for stars with  $v \sin i$  lower than this value it is not possible to determine the rotational velocity but only an upper limit.
- **Blending**: The typically high rotational velocities of most of the stars in our sample make it very difficult to apply the method to isolated lines. Blended features were used instead. A careful inspection using synthetic spectra was performed to avoid contamination in the Fourier transform due to the intrinsic profile of the blended features (Figures 3,4).

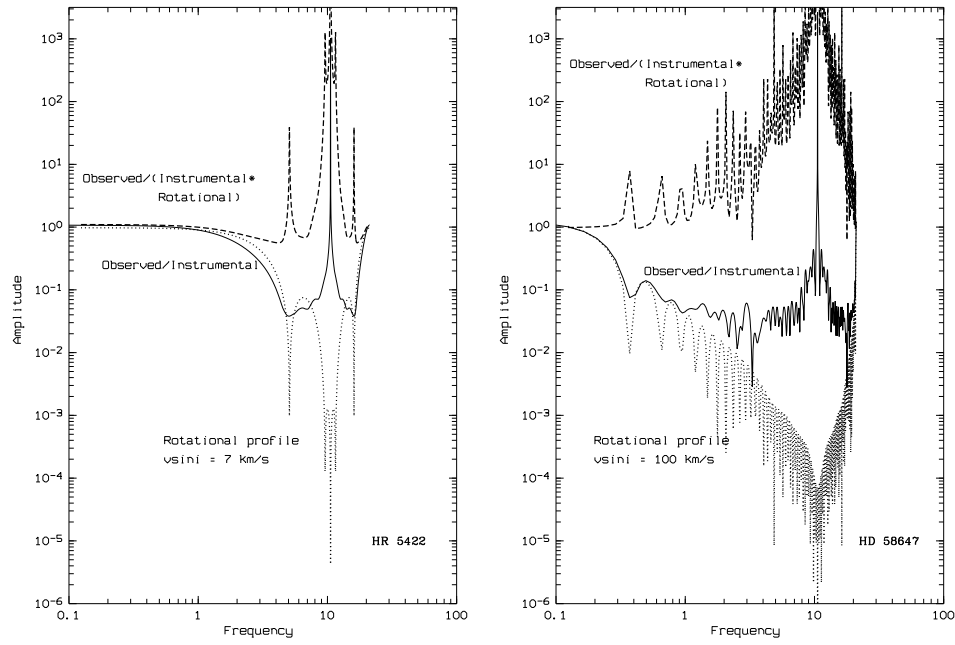


Figure 2. Removal of rotational profile for slow (left panel) and fast rotators (right panel).

## 5. Conclusions

The suitability of the method proposed by Gray (1992) to derive rotational velocities has been demonstrated in this paper. In addition to this, the presence of other sources of broadening, like macroturbulence, can be also estimated for slow rotators. The characterization of the different type of objects of the EXPORT sample according to their rotational velocities and the implications in the stellar evolution is part of a currently ongoing work.

## References

- Bruning, D.H. 1981, *ApJ*, 248, 274  
 Gray, D.F. 1992, in *The observation and analysis of stellar photospheres*, ed. Cambridge Univ. Press, 368  
 Sletteback, A., Collins, G.W., Boyce, P.B., White, N.M., Parkinson, T.D. 1975, *ApJS*, 29, 137  
 Solano, E., Fernley, J. 1997, *A&AS*, 122, 131  
 Tonry, J., Davis, M. 1979, *AJ*, 84, 1511

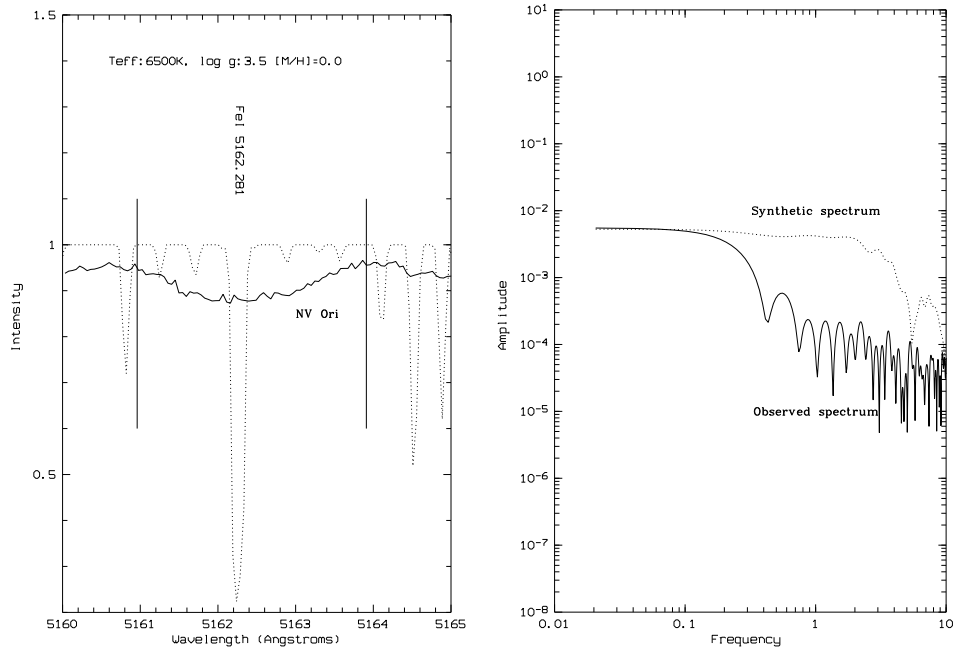


Figure 3. Influence of the intrinsic profile of blended features in the Fourier transform. The observed spectrum (solid line) is compared to a synthetic spectrum with similar physical parameters and  $v \sin i = 0$  (dotted line). Assumed line edges are also marked. The contribution of the intrinsic profile lies at high frequencies not affecting the  $v \sin i$  determination.

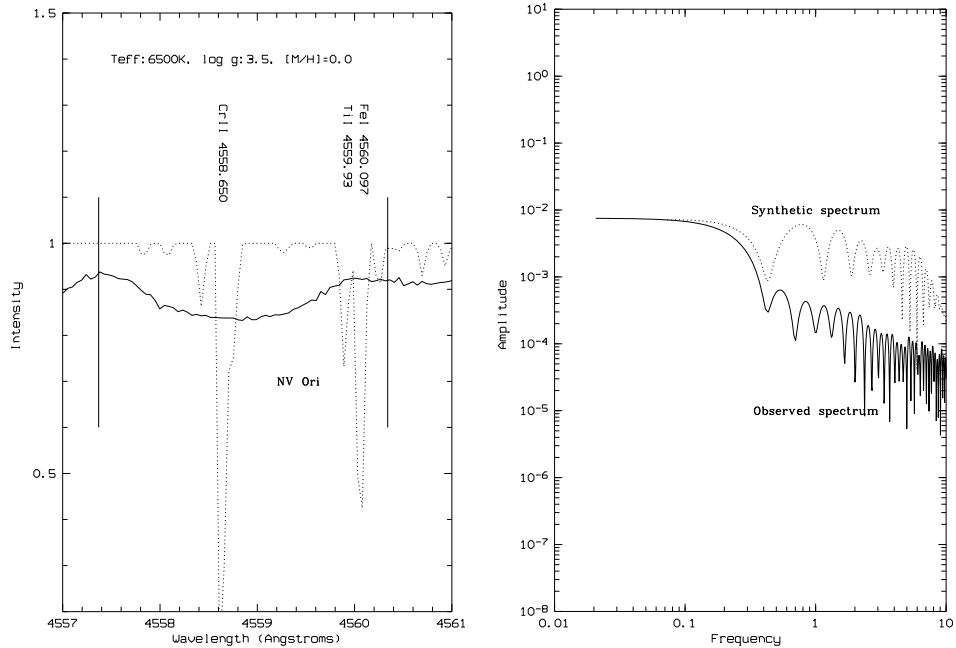


Figure 4. Similar to Fig. 3 but, in this case, the intrinsic profile produces a spurious minimum in the Fourier transform of the observed spectrum which may lead to a wrong  $v \sin i$  determination.

Table 1. Projected rotational velocities of program stars. The number of lines used in the analysis are given in parentheses. “\*” indicates the presence of macroturbulence as additional source of broadening.

Target	Type	$v \sin i$ (km/s)	
		Measured	Adopted
BH Cep	H Ae/Be	97 ± 8(8); 97 ± 5(7); 98 ± 6(11)	
49 Cet	Vega-like	183 ± 9(4); 187 ± 4(3)	
24 CVn	A shell	168 ± 6(6); 177 ± 5 (3)	
T Ori	H Ae/Be	175 ± 14(9)	
BF Ori	H Ae/Be	34 ± 3(33); 33 ± 6(14); 36 ± 5(10); 44 ± 4(8)	
CO Ori	UXOR	60 ± 9(21); 68 ± 5(6) ; 61 ± 8 (9)	
HK Ori	UXOR	28 ± 6(34)	
NV Ori	H Ae/Be	81 ± 8(19)	
RY Ori	H Ae/Be	66 ± 6(19)	
UX Ori	UXOR	165 ± 4(3); 213 ± 11(3)	
CQ Tau	H Ae/Be	105 ± 5(6)	
RY Tau	T Tauri	49 ± 7(3); 56 ± 6(8); 57 ± 6(8); 55 ± 10(10)	
HR 419	B9 V	162 ± 14(7)	
HR 4227	A-type	152 ± 6(4); 129 ± 8(5)	
HR 4757 B	PTT	5.2 ± 0.7(35)	
HR 5422	A-type	7.6±0.7(52); 7.2 ±0.8(45)	
HR 9043	βPic-like	192 ± 22(4); 218 ± 11(3)	
HD 23362	Vega-like	6± 0.7(25)	
HD 31293	H Ae/Be	97 ± 20(8)	
HD 31648	H Ae/Be	111 ± 8(8); 87 ± 13(8);101 ± 9(5);96 ± 13(8)	
HD 34282	H Ae/Be	132 ± 15(12); 125 ± 16(6)	
HD 34700	H Ae/Be	48 ± 3(11); 30 ± 8(11)	
HD 58647	H Ae/Be	119 ± 5(3); 117 ± 8(3); 116 ± 12(2)	
HD 109085	Vega-like	66 ± 5(29); 71 ± 4(9); 67 ± 4(13); 68 ± 3(7)	
HD 123160	Vega-like	8 ± 1.5(13)	
HD 141569	H Ae/Be	283 ± 10(3)	
HD 142666	UXOR	74 ± 4(7); 72 ± 4(14); 71 ± 4(21); 75 ± 4(16)	
		73 ± 3(11); 70 ± 3(13)	
HD 142764	Vega-like	7 ± 3 (34)	
HD 144432	H Ae/Be	81 ± 6(10); 85 ± 11(7) ; 88 ± 8(9); 89 ± 9(8)	
HD 163296	H Ae/Be	134 ± 15(7)	
HD 199143	F-type	159 ± 17(7); 154 ± 9(6)	
HD 233517	Vega-like	17 ± 3(5); 16 ± 2(6); 15 ± 2(24)	